Connecting the Physics of Stars, Galaxies and the Universe

FAME Astrometry & Photometry and NASA's Research Themes

Version 2.0, April 8, 2003

Rob P. Olling[1,2]

[1]US Naval Observatory, [2]USRA

1. Description of the FAME Mission

1.1. Science Objectives

The scientific return of the FAME astrometric mission has been well-documented by the FAME team (FAME 2000–2002), and include: 1) the definitive calibration of the absolute luminosities of the standard candles (Sandage & Saha 2002); 2) the physical characterization of solar neighborhood stars of most types, 3) the frequency of companions ($M \gtrsim 80 M_J$) of solar-type stars; 4) stellar variability; 5) the binarity frequency; 5) stellar evolution and structure will be checked in great detail in nearby star clusters and visual astrometric binaries; 6) distances and proper motions allow, for the first time, a detailed study of the ages and kinematics of the youngest known stars in star forming regions; 7) the survey nature of FAME ensures that a large number of stars become available to probe the potential of the Milky Way in both the radial and vertical directions (rotation curve and disk mass). The implications of the FAME mission are so diverse that new applications of its accurate astrometric and photometric data are constantly being reported in the literature: 8) improving and extending the reference frame to $R \sim 18$ (Salim, Gould & Olling 2002); 9) exploring the low-luminosity stellar population in the immediate solar neighborhood [$d \lesssim 50$ pc; Salim, Gould & Olling (2002)]; 10) optimal methods for detecting (low-mass) companions via astrometric techniques [Eisner & Kulkarni (2001, 2002)]; 11) unraveling details in the dynamics of extra-solar planetary systems (Chiang, Tabachnik, & Tremaine 2001); 12) the history of stellar encounters with the Solar system (García-Sánchez *et al.* 2001); 13) the structure and dynamics of young star clusters (Adams *et al.* 2001); 14) determining the formation history of the Galactic halo (Helmi & de Zeeuw 2000); 15) distance determination to external galaxies (Gould 2000; Olling & Peterson 2000).

Given its wide and profound ramifications, it comes as no surprise that the FAME mission is well-received across the astronomical community. To date we found already twelve papers in the refereed literature that discuss how FAME data can further specific science goals [Salim, Gould & Olling (2002); Sandage & Saha (2002); Bailer-Jones (2002); Eisner & Kulkarni (2002); Adams *et al.* (2001); Chiang, Tabachnik, & Tremaine (2001); Eisner & Kulkarni (2001); García-Sánchez *et al.* (2001); Han, Black, & Gatewood (2001); Olling & Merrifield (2001); Gould (2000); Helmi & de Zeeuw (2000)].

1.1.1. Characterization of the FAME catalog

We characterize the contents of the FAME catalog in two ways. First, we estimate the fraction of Galactic disk stars that enter the FAME catalog. We assume that the Sun is located 7.5 kpc from the Galactic center, and approximate the distribution of stars in the Milky Way (MW) as radially exponential with a scalelength of 2.5 kpc. With these assumptions, the

probability of finding a star at distance d kpc of the Sun is found to be: $P(d) \sim 0.405 \, d_{kpc}^{2.09}$ %. In other words, a particular type of rare star has a fair chance to lie within d kpc of the Sun if the total number of those stars, $N_{MW}^{*,tot}$, in the Galaxy exceeds $100/P(d)$. For $d = 1$ kpc, we derive $N_{MW}^{*,tot} \sim 250$. Such a star will be in the FAME catalog if its absolute magnitude is brighter than $M_V \sim 4$, that is to say, brighter than a late-F main-sequence (MS) star. Thus many rare stars (with short evolutionary timescales) will be well-represented in the FAME catalog. For example, planetary nebulae (PNe) have absolute luminosities of $M_V \sim 6$, for about 30,000 years before they cool down too much to be able to ionize their nebula. The Galaxy may contain 30,000 PNe (Allen's Astrophysical Quantities 2000), so that we expect about 42 planetaries within 600 pc, while at least 34 known planetaries lie within this distance (Pottach 1996). Other rare and interesting objects that lie within the FAME distance horizon are hard X-ray binaries with bright optical counterparts such as 3A0535+26, Vela X-1, SS Cyg and the black-hole candidate Cyg X-3 (Allen's Astrophysical Quantities (2000), Table 9.8).

Second, we describe the FAME catalog with the aid of a star-count model. This is a fairly simple model. We copy the local densities of the O, B, A, F, G, K and M types for main-sequence stars and "average giant-branch" stars from (Binney & Merrifield 1998). We also include an estimate for the space density of Cepheids. We assume the space density of Cepheids to be 0.03 times that of their progenitors (B-stars)[1].

We then re-normalize the multiply (by 1.86) the densities of the O–K stars to match the total number of O–K stars in the NSTARS database within 25 pc.

We include a vertical density gradient, where we use "standard" values for the exponential scaleheight, as a function of spectral type and luminosity class (h_z=40, 100, 200, 280, and 300 pc for O/B, F, G, K/M stars, and 250 pc for the giants).

Finally, we do not include any latitudinal dependence of the extinction. Using this simple model, we determine the total number of stars brighter than $R = 15$, as well as the distribution among the types and classes. This model reproduces fairly well the total number of stars in the Tycho-2 catalog, as well as the "star-counts" of the Galaxy model employed for the GAIA mission. However, at brighter magnitudes ($V = 7$), our simple model over-predicts the number of stars by about a factor of two with respect to the Hipparcos numbers. We ascribe this to our primitive implementation of the extinction corrections.

To estimate the stellar content as a function of astrometric precision, we simplify matters further (see footnote 3). We present the results in Table 1. In the first three columns of this

---

[1] A factor of ten arises from the ratio of the MS and Cepheid phases (60 Myr versus 6 Myr), and we further reduce the Cepheid density by an arbitrary factor of three

table we enumerate as a function of spectral type, an average absolute magnitude for that type and the distance out to which such stars have an apparent magnitude equal to the limiting magnitude of the FAME catalog ($R = 15$). For these calculations we assume that the extinction along the line of sight equals 1.4 magnitude per kpc, on average. Each spectral type samples a different volume around the Sun. Cepheids[2] and B-type stars can be seen halfway across the Galaxy, while M-stars are only visible in the immediate solar neighborhood. The "rest" category comprises many interesting stars such as pre-MS stars, white dwarfs, horizontal branch stars, RR Lyrae, and supergiants, but this category is dominated by K giants. We therefore assigned it an absolute magnitude of $M_V = 0.6$ (typical for the Red Clump region). Note that the modal star in the FAME catalog will be of spectral type G.

Columns 5–9 (10–14) list the limiting distance, limiting magnitude and the number of stars in the thin-disk, thick-disk and spheroid for two samples with distance errors better than 10% (0.5%)[3]. Note that the large number of stars in the thick disk and spheroid components: 1×10^6 and 31,000 for the sub-sample with 10% astrometric errors (8,300 and 206 for the 0.5% sample).

1.1.2.   Science at $\pi/\delta\pi = 10$

To avoid the pitfalls of negative parallaxes, astronomers typically limit themselves to objects with well-measured ($\geq 10\sigma$) parallaxes. The characteristics of the 10% sample are presented in columns 5–9 of Table 1. This sample is about 900 times larger than Hipparcos'

---

[2]For the Cepheids we took the absolute magnitude that corresponds to a 6-day period. The duration of the Cepheid phases depends strongly upon mass. For a "typical" mass of 6 $M_\odot$, we estimate a total lifetime of 6 Myr, or about 10% of the main-sequence lifetime of their progenitors (B-type stars). Conservatively, we assume a detection rate of 30%, to arrive at $N_{Cep} \sim 0.03 N_B$. **Note that the known density of Cepheids is roughly 30 times smaller. A possible explanation might be that A) the time-scale estimate is wrong, B) that Cepheids in the instability strip only spend part of the time in a high-amplitude pulsation mode. A possible example might be Polaris which sits right in the middle of the instability strip but has hardly discernible pulsations, as well as a time-varying pulsation amplitude: both for unknown reasons. At any rate, I don't use the number of Cepheids very much in this document anyway.**

[3] To estimate the number of stars with given absolute magnitude, we assume that the space density is constant within $\frac{1}{2}$ of the vertical scaleheight (h_z), and zero at larger heights above the plane. Thus, the number of stars increases proportional to d^3 while $d \leq h_z/2$, and proportional to d^2 for $d > h_z/2$. We assumed, h_z=250, 1000, 10000 pc for the thin disk, thick disk and spheroid, respectively. Note that due to the larger scaleheight of the thick disk and spheroid, the sampled volume is substantially larger for thick-disk and spheroid stars than for thin-disk stars. We assume that the local number density of thin-disk, thick-disk and spheroid comprise 95.9%, 4% and 0.1% of the total number density, respectively. **In the mean time, I have significantly improved my star-count model. So take the numbers in this document with a grain of salt. The numbers for the Bessel mission are generated with this new, improved model.**

magnitude limited 10% sample of about 14k stars (Dehnen & Binney 1998). Thus, to first order, any property of an ensemble of stars will be determined $\sqrt{900} = 30$ times better with the FAME catalog than with the Hipparcos catalog. Stated in another way: any property that could only be marginally determined with Hipparcos data ($\pm 100\%$), can be determined at the 30σ level employing the FAME catalog.

For example, Crézé *et al.* (1998) used Hipparcos parallaxes and proper motions for ∼2,500 A and F-type stars within 125 pc to determine the value for the the total mass density in the Galactic plane (the Oort limit) to $\pm 19\%$. The FAME mission would yield 986 times more stars: a potential improvement by a factor 32. For this analysis, mostly stars close to the Galactic plane would be used, so that their unknown radial velocities hardly contribute to the desired vertical component of the space velocity.

The determination of the rotation curve of the Milky Way is currently very difficult. For example, the rotation curve inferred from the Cepheids and the neutral hydrogen (H I) differ substantially (Dehnen & Binney 1998). It may be that the analysis of the H I is incorrect, or that the interpretation of the Cepheid data is compromised by the fact that the analysis relies on parametric models (Olling & Merrifield 1998), and/or systematic effects in the Period-Luminosity (PL) distances. The Hipparcos calibration of the Cepheid distance scale has helped a lot by providing distances based on the PL relation (Feast & Whitelock 1997). However, these PL-distances are difficult to use because they depend on many intermediate steps, so that the estimated errors are hard to interpret. Furthermore, metallicity corrections have not been incorporated in this PL calibration so that the errors, in all likelihood, contain a dependence upon Galactocentric radius. This is a highly undesirable feature for the purpose of the determination of the rotation curve. Currently, it is virtually impossible to test for systematics in the PL relation: one needs FAME parallaxes for that purpose. We estimate that the FAME mission may discover 12,000 new Cepheids, and ∼1,500 of these Cepheids will lie within 2 kpc of the Sun. Thus, the FAME Cepheid sample[4] will revolutionize our ability to determine the Galactic rotation curve, in particular when radial velocities are also obtained.

In fact, this sample is fairly large and dense [3 stars per $(100 \text{ pc})^2$], so that deviations from circular motion may be reliably determined [5]. Because of their low velocity dispersions,

---

[4]The progenitor B-star sample is much larger, and would hence be even better than the Cepheids. However, it is easier to determine the radial velocity for F&G-type Cepheids than for B stars. We therefore surmise that the Cepheids will be used rather than the B-star sample. Furthermore, the Cepheids can be seen to somewhat larger distances than B stars.

[5]A peculiar velocity of 10 km s^{-1} at $d \leq 2$ kpc translates to a peculiar proper motion of $\gtrsim 1$ mas yr^{-1}, or $\gtrsim 20\sigma$

young stars such as Cepheids are very suitable to measure perturbations in the potential[6]. For example, the strength of the bar and the mass distribution of spiral arms can determined. Also, if a substantial dark-matter clump has settled in the solar neighborhood, it will betray its presence kinematically.

Due to Hipparcos' small limiting distance of ∼100 pc, the vertical structure of the disk could hardly be probed. The FAME data set on the other hand allows one to generate a distance limited sample of K giants that extends well into the thick disk. Table 1 shows that we can expect about 2.4×10^6 K-giants out to 1,200 pc. Since the scaleheights of the thin and thick disks are about 250 and 1000 pc, respectively, the FAME K-giant sample is ideally suited to settle the issue of the relative importance of the two disk components. However, some accommodation is necessary for age variation among giant stars. Since stars of (virtually) all masses will spend a considerable fraction of their lifetime on or near the red-giant branch, the current-day giant branch is populated by stars of all masses, and hence ages[7]. However, if one assumes a constant star-formation rate throughout the history of the Milky Way and a universal initial mass function, then the stellar masses on the giant branch will be similar to the masses of the progenitor that just now reached the giant branch(i.e., 1 $M_\odot$ stars if the MW disk is 11 Gyr old[8]).

The K-giant sample can also be used to derive the total disk mass via kinematical analysis [e.g.,Bahcall (1984a,b); Kuijken & Gilmore (1989a,b); Flynn & Fuchs (1994)]. However, the asymmetric drift, the velocity dispersion and the vertical scaleheight gradually increase as with time, so that the analysis of K giants is complicated by their age-mix[9]. To date, such sophistication was unwarranted due to the low precision of the available data. For optimal results, FAME-based analyses will need to consider the stellar ages. Therefore, the FAME data itself is essential but not sufficient to determine ages of K giants[10]. Similar problems

---

[6]The responsiveness of a population to perturbations in the potential is inversely proportional to the square of the velocity dispersion of that population (Mayor 1974):$V_{pec} \propto 1/\sigma_{pop}^2$.

[7]For example, from the data presented by Binney & Merrifield (1998), a 69 Myr old 6 $M_\odot$ star (B6 on the main sequence) has just now arrived on the giant branch: just like a 357 Myr old 3 $M_\odot$ star (B9/A0 on the MS), a 2.6 Gyr old 1.5 $M_\odot$ star (F2 on the MS) or a 11 Gyr old 1 $M_\odot$ star (G2 on the MS). These ages can be substantially shorter for lower metallicity stars ($\leq$70% shorter for [Fe/H]=-1.75).

[8]Given the assumption stated, the relative frequency on the main sequence as compared to that on the giant branch for masses of 1.0, 1.5, 2.0, 3.0, 4.0, 6.0 and 9.0 $M_\odot$ are: 1.0, 1.09, 1.88, 11.1, 20.4, 37.2 and 58, respectively.

[9]Analyzing the sample of giants without accommodating for age differences is akin to analyzing all main-sequence stars together. Given the age-velocity relation (Dehnen & Binney 1998), such would be an undesirable endeavor.

[10] The observed flux and distance yield the absolute luminosity. Taken together with the effective temper-

will arise for any type of star for which the lifetime is a considerable fraction of the age of the Galactic disk.

To conclude, the paucity of the Hipparcos astrometric catalog severely limits our ability to make substantial progress in our understanding of many dynamical processes that have been, and are currently shaping our Milky Way. This has been the usual situation for centuries. However, as soon as FAME-like astrometric data becomes available, advances in our understanding will be limited by the scarcity of auxiliary information, most notably stellar age, metallicity and gravity. This additional information needs be extracted from supplemental, high-quality photometric and/or spectroscopic data.

1.2. Science at 50 μas

Table 1 shows that FAME will determine the distances of roughly 231,000 stars closer than about 100 parsec with an accuracy of 0.5% (50 μas). Contained in this 0.5%-sample are $\sim$2,600 A-type, $\sim$27,000 F-type, $\sim$87,000 G-type, $\sim$58,000 K-type and $\sim$45,000 M-type MS stars. Among the 0.5%-sample, there are about 4% thick disk stars (8,300) and 0.1% halo stars (206). Most of these stars have magnitudes R=10–12, and are thus rather suitable for high-resolution, ground-based, follow-up spectroscopy.

This sub-sample is FAME's premier data product, where its importance stems from the astonishing, almost laboratory-quality, accuracy. The availability of accurate data has huge implications for the physics of stars (*astro*physics), and all derived branches of astronomy (i.e., all of astrophysics). After all, the stars are the stepping stones towards an understanding of the universe.

1.2.1. Stellar Astrophysics

Our current understanding of stars and stellar atmospheres is rather basic in the sense that the gross features of stellar evolution and atmospheres are understood, while many important details such as convection or abundance determination remain unsatisfactory. Sneden *et al.* (1995) point out that sensitive, high-resolution spectroscopy ($S/N \geq 100$, $\lambda/\delta\lambda \gtrsim 60,000$) is required for accurate abundance analysis, which would advance many many fields of Galactic and extragalactic research. However, as pointed out for the K-giant case in section 1.1.2, FAME data in combination with spectroscopy allows for a precise deter-

---

ature and Stefan-Boltzmann's law, the radius can be determined. The mass of the star then follows from a spectroscopic or photometric determination of the surface gravity. Evolutionary models then yield the age of the star, given its observed metallicity.

mination of absolute luminosities[11], temperatures, radii, surface gravities and masses of the stars (see footnote 10). It is then up to the theories of stellar evolution to find a star with the right mass (M), luminosity (L), temperature (T_{eff}), radius (R), metallicity (Z) and age (τ) to fit the observed values. Given our fairly basic knowledge of the physics of stellar interiors and atmospheres[12], we should be pretty amazed if the theoretical and observational parameters fit to within the errors. Extrapolating from the Hipparcos experience (Lebreton 2001), we anticipate that the availability of precision FAME data will spur a burst of theoretical investigations which will produce major advances in astrophysics.

For example, one very important parameter is inaccessible to direct observations for most types of stars. This parameters is the Helium abundance (Y) of the star, and can be determined by matching up the observational and theoretical M, L, T_{eff}, R and Z values. The dependence of luminosity on Y (Lebreton et $al.$ 1999) can be inverted to read $\delta Y \sim 1/300 \, \delta L_\% \sim 2/300 \, \delta d_\%$, so that a distance error ($\delta d_\%$) of 0.5% corresponds to an error of 3×10^{-3} in Y[13]. The analysis of Lebreton et $al.$ (1999), performed on the best 33 Hipparcos stars goes some way towards the eventual goal outlined above: they already uncovered evidence for the importance of variations in Y, non-LTE effects in abundance analyses and sedimentation of heavy elements. One application of this procedure is to determine the evolution and the primordial abundance of Helium, which is an important boundary condition for Big Bang models. Another very interesting application would be to look for variations in the pre-Galactic variation of the Helium abundance among the members of the different halo streamers. Any such variation may indicate in-homogeneous Big Bang nucleosynthesis.

1.2.2. Expected Accuracies for Stellar Masses and Ages

Combining Newton's law of gravitation with the Stefan-Boltzmann law, the stellar mass is given by: $M = g \, L/(4\pi \, G \, \sigma \, T_{eff}^4)$, with g, G and σ the surface gravity, Newton's constant and the Stefan-Boltzmann constant, respectively. The error in the stellar mass is then given

---

[11]Note that a 1% luminosity determination also requires a determination of the extinction to 0.01 magnitude. Given that the expected A_V is of order 1 mag/kpc, a star at 100 pc has $A_V \sim 0.1$. Thus we require an extinction determination with a precision of only 10%.

[12] To quote R. Kurucz (2001): A) "We do not know how to make realistic model atmospheres; we do not understand convection," B) "We do not understand spectroscopy; we do not have good spectra of the Sun or any star," C) "We do not have energy distributions for the Sun or any star," D) "We do not know how to determine abundances; we do not know the abundance of the Sun or any star," and so forth.

[13]Note that such determinations of Y are independent of any $Y(Z)$ relation: the classical way to determine Y for long-lived cool stars [e.g., Binney & Merrifield (1998)].

by:

$$\left(\frac{\Delta M}{M}\right)^2 \quad \sim \quad [2.3\Delta log(g)]^2 + \left(\frac{\Delta L}{L}\right)^2 + \left(\frac{4\Delta T_{eff}}{T_{eff}}\right)^2 \tag{1}$$

Given the difficulties in deriving accurate atmospheric parameters [Kurucz (2001) and see footnote 12] it is not surprising that there exists a rather large variation among the reported values of $log(g), T_{eff}$ and $[Fe/H]$, even among publications that employ high-resolution spectroscopy. For Sun-like stars, Soubrian, Katz & Cayrel (1998) find an average RMS difference among the reported values for $log(g)$, T_{eff} and $[Fe/H]$ of 0.25 dex, 2% and 0.1 dex, respectively. Note that similar uncertainties can be achieved from low-resolution spectroscopy and even intermediate-band photometry, provided that the signal-to-noise ratio is large enough [e.g., Bailer-Jones (2000, 2002); Olling (FTM2001-07); Snider $et\ al.$ (2001)]. The resulting uncertainty in mass is about 59%, where the error is dominated by the surface gravity determination. Clearly, so as to yield relevant age estimates, the errors on $log(g)$ (and T_{eff}) have to be substantially reduced. This will require a major effort from the theoretical and observational communities. The FAME contribution is to eliminate any uncertainty associated with absolute luminosity.

To understand why such efforts are worthwhile, consider that a distance uncertainty of 0.5% corresponds to a luminosity error of 1%. This luminosity resolution translates in an uncertainty with which stellar ages can be estimated. We determine the rate of luminosity evolution from the Bertelli $et\ al.$ (1994) isochrones. Between the zero-age main sequence and zero-age giant branch phases, the rate of luminosity evolution can be approximated by:

$$\Delta L/L \sim -0.17 + 0.32\,M/M_\odot \sim 0.1 + 0.02\,L/L_\odot \sim 0.24 - 0.106\,\log\left(\tau_{MS}\right)\ \pm 0.05[\mathrm{Gyr}^{-1}] \tag{2}$$

where τ_{MS} is the "main-sequence lifetime"[14] in Gyr. The three forms of luminosity evolution result in the fractional rate of luminosity evolution being largest for the most massive stars. That is to say, for the stars that have shortest MS lifetimes and largest MS luminosities. For example, the rate of luminosity evolution for an A0V star of mass 2.5 $M_\odot$ equals 63% per Gyr, as compared to $\sim$13% per Gyr for the Sun. For sun-like stars, a 10% (1%) luminosity resolution leads to an age discrimination of roughly 770 (77) Myr.

1.2.3. Fundamental Stellar Parameters from Binaries

The most important parameter that determines the internal structure and evolution of a star is its mass. Currently, stellar masses can be determined with a precision of $\gtrsim$ 1-2%.

---

[14]Here we define the MS lifetime as the elapsed time between the zero-age MS and the zero-age giant branch (roughly points 1 and 5 in figure 5.2 of Binney & Merrifield (1998)).

As of 1991, only 44 such systems have been analyzed [88 stars among which are only *four* main-sequence G stars, Andersen (1991)].

Given sufficient spectroscopic observations, detached double-lined eclipsing binaries (DEBs) are well-suited for accurate mass, radius and gravity determinations. When distances and extinctions are determined at the same level, detailed checks on the interior structure and evolution of stars are possible. If the temperatures of the stars can be determined from photometry and/or spectroscopy, rather accurate distances *throughout the Local Group of galaxies* can be determined [e.g., (Paczyński 1996; Wyithe & Wilson 2002)][15]. Such analyses are currently being used to map out the internal structure of the Magellanic Clouds and the distance to M 31 [e.g., Kaluzny *et al.* (1998); Fitzpatrick *et al.* (2002), and references therein].

Eclipsing Binaries

Similar analyses would be very worthwhile for the DEBs found in the FAME catalog. The OGLE and HIPPARCOS experiments find that about 0.8% of all stars are DEBs with periods of about 1 day in the very different environments of the Galactic bulge and the solar neighborhood. Extrapolating these numbers to the FAME catalog, we expect to find of order 400,000 new DEBs. Roughly 10% (40k) of these DEBs will be brighter than $R = 12$. For such short period DEBs, FAME's scanning geometry ensures the detection of 14±8 eclipses per DEB, in the average (see section 1.4 below). Convolving the period distribution of binary stars [Duquennoy & Mayor (1991), hereafter DM1991] with the probability that FAME will measure at least 2 eclipses, we estimate that about **3.2% of stars will be in eclipsing systems, with a modal value of 5.3 days. This results in a list of** 1.3×10^6 **systems**[16], so that ground-based photometric and spectroscopic follow-up for the FAME DEBs will be extremely efficient. The large number of DEBS will ensure that they will be found among stars of all masses and ages, provided that the particular phase of stellar evolution is long enough to produce 1/0.008=125 objects in the FAME catalog.

Alternatively, the observed astrometric wobble, in combination with the eclipse photometry can be used to determine the stellar parameters. To our knowledge, there are no published investigations that explore this topic. Below we develop an order-of-magnitude estimates of the utility of this approach.

While the radial velocity method is most sensitive to short-period systems, the amplitude

---

[15] However, over-contact binaries should perform even better because these systems have far fewer free parameters since both stars have identical T_{eff}, $[Fe/H]$ and $log(g)$ [R. Wilson, (2002) private communications].

[16]**This is actually wrong: the percentage must equal 0.86%, so that all numbers in the remainder of this document regarding the number of DEBs need be multiplied by 0.27.**

of the astrometric signal [the semi-major axis (a_A)] *decreases* with period, and is hence intrinsically less suited to study short-period systems:

$$a_A \;=\; \Pi\,[(M_1 + M_2)\,T^2]^{1/3} \;=\; \frac{100}{d_{10}}[M_T\,T^2]^{1/3} \quad \text{[mas]} \tag{3}$$

Here a_A and the parallax (Π) are expressed in in the same unit (e.g., mas), while d_{10} is the distance in units of 10 pc. The sum of the masses (M_T), as well as the primary (M_1) and secondary (M_2) are in units of solar masses and the orbital period (T) in years.

However, for unresolved systems, one only observes the motion of the photocenter. To determine this photocentric wobble, consider that a equals the sum of semi-major axis of the primary and secondary $(a_A = a_1 + a_2)$, while $a_1 = a \times M_2/M_T$ and $a_2 = a \times M_1/M_T$. Further, if L_T equals the sum of the light from the primary (L_1) and secondary (L_2), the semi-major axis of the photocenter (a_P) is given by:

$$a_P \;=\; \frac{L_1\,a_1 - L_2\,a_2}{L_T} \;=\; \frac{100}{d_{10}}\left(\frac{T}{M_T}\right)^{2/3}(\ell_1\,M_2 - \ell_2\,M_1) \quad \text{[mas]} \tag{4}$$

with $\ell_i = L_i/L_T$. In the section on astrometric binaries below, we find that the maximum astrometric signal for astrometric binaries occurs for $M_2/M_1 \sim 0.9$. For the lower main sequence, where $L \propto M^5$ Binney & Merrifield (1998), a 10% chance in mass results in a 50% change in luminosity. In this case, we can re-write eqn. (4) to read:

$$a_{P,90\%} \;\approx\; \frac{0.9}{d_{25}}[M_1\,T_{10d}^2]^{1/3} \quad \text{[mas]} \tag{5}$$

where we have expressed the period in units of 10 days, and the distance in units of 25 pc. Numerically, eqn. (5) is about 6 times smaller than the actual semi-major axis given by eqn. (3). About 1% of stars are in eclipsing systems with periods between 5 and 15 days (DM1991), or about 100 systems within 25 pc. Their photocentric wobble can be determined at the $\sim 35\sigma$ level. Furthermore, about 70% of these systems will have the eclipses confirmed by FAME photometry. However, the fraction of almost-equal mass binaries is fairly small, so that hardly any eclipsing systems will result in high-quality data.

Thus, FAME *astrometry* will make a limited contribution to the study of eclipsing binaries. However, FAME's *photometry* will make a major contribution to this very important field because of the discovery of order 1.3×10^6 new DEBs. 10% of those are bright enough for sensitive, high-resolution ground-based follow-up.

Visual Binaries

Equation 3 is only valid for systems where the orbit is resolved. For such "visual binaries," all orbital elements can be determined with good accuracy, provided that the distance is

well-determined, and the orbital period is not too long. The most comprehensive catalog of double stars, the "Washington Double Star catalog" [WDS,Mason *et al.* (2001)], contains just 2 systems that would qualify as FAME visual binaries. However, the WDS is rather incomplete below $V = 7$, so that the final FAME catalog is expected to contain more such systems:[17]

$$N'_{VB} \quad \sim \quad 25 \, M_T \, T^2 \; . \tag{6}$$

Assuming a 1 $M_\odot$ system, and integrating the product of eqn. (6) and the probability-density distribution for periods of binary stars (Duquennoy & Mayor 1991), we arrive at a total number of $N_{VB} \sim 310$ visual binaries with orbit solutions. These F–G visual binaries all lie within 50 pc, with distance uncertainties $\sim 0.5\%$, and hence masses to three times that precision, or 1.5%. The FAME catalog of visual binaries will comprise 310 systems with 620 F–K MS stars (77 GV stars), a 7-fold (19-fold) increase with respect to the current 1% sample [c.f., Andersen (1991)].

Astrometric Binaries

We have simulated the efficiency with which FAME can detect astrometric binaries, where we assumed that both stars are on the main sequence with masses between 0.2 and 39 $M_\odot$. The luminosities for both components are determined according to their MS luminosities, as tabulated by Binney & Merrifield (1998). The results are presented in Figure 1, where we contour the semi-major axis of the photocenter as a function of the mass of the primary and secondary. The actual values plotted are valid for a distance of 100 pc, a period of 1 year and are scaled by FAME's astrometric accuracy of 50 μas. The contour plot may be scaled to different parameters by multiplication by $100/d_{pc} \times T^{2/3}/(1\,yr) \times (50\mu \text{as}/\delta x_0)$. The masses and luminosities are equal on the diagonal line. In most parts of parameter space ($M_2/M_1 \leq 0.95$), the photocentric wobble is easily resolved. For example, for $M_1 = 10$ and $M_2 = 0.2$ ($\Delta m \sim 10.4$ mag), the secondary is detectable at the 10σ level. Likewise, a 0.01 $M_\odot$ secondary around a 1 $M_\odot$ star yield a 20σ detection for $\Delta m \gtrsim 8$ mag. Figure 1 shows that the best detection of binarity occurs for mass ratios of about $\frac{1}{2}$ and signal-to-noise ratios of 50–200. At 300 pc, 5 year binaries are detected at about the same significance as 1 yr binaries at 100 pc.

---

[17] Visual binaries will be well-observed when the semi-major axis exceeds one-half times the pixel size (separation ≥ 1 pixels; $a_A \geq 0.147$"). Based on Hipparcos data, Söderhjelm (1999) shows that good orbital solutions are possible when the period is smaller than four times the mission length, or 20 years for FAME. From eqn. (3) it then follows that the distance out which a star can be recognized as a visual binary (d_{VB}) equals: $d_{VB} = M_T^{1/3} T^{2/3}/a_{A"}$, with $a_{A"}$ in arcsec. Thus, the volume sampled equals $V_{VB} = 4/3\pi M_T T^2/a_{A"}^3 \sim 1,314 M_T T^2$ pc^3. Given a local density of F–K MS stars of 1.88×10^{-2} per pc^3 [cf., Binney & Merrifield (1998), table 3.19], the number of stars that can be searched for visual binary equals $\rho \times V_{VB}$.

Thus, FAME will detect virtually all binaries with $0.5 \lesssim T_{yr} \lesssim 5$ around all 236,000 star systems within 100 pc from the Sun. Note that the determination of orbits will only succeed for the more robust measurements. FAME will be better at separating orbits with periods of about 1 year from the parallactic motion than Hipparcos or GAIA because FAME provides about twenty times more observations than Hipparcos or GAIA.

1.2.4. Astrometric Detection of Planets

If the secondaries are "dark" (e.g., brown dwarfs or planets), the photocentric major axis is given by the semi-major axis of eqn. (4), with $L_2 = 0$:

$$ a_{P,\sigma} = 2.34 \left(\frac{T_{5\,yr}^{2/3}}{d_{25\,pc}} \right) \times \left(\frac{M_P}{(M_T^\odot)^{2/3}} \right) \times \left(\frac{50\mu as}{\delta x_0} \right) \tag{7} $$

where we expressed the mass of the planet (M_P) in units of Jupiter ($M_J \sim 0.001 M_\odot$), the distance in units of 25 pc, and a_{Phot} in units of the astrometric accuracy. We present the results in Figure 2. The dotted lines of represent lines of constant constant confidence $N \times \sigma$, for the case of a 5 year orbital period, where the N values are associated with the contours. The thick lines are the 10σ detections for periods of 1,2,3,4 and 5 years, from top to bottom.

To estimate the total number of detectable planets, we solve eqn. (7) for the distance and determine the volume accessible to to stars with a given planetary mass and period:

$$ V_P = \frac{4}{3}\pi d^3 \sim \frac{3,350}{(\delta x_{0,50}\, a_{P,\sigma})^3} \times \frac{T_{yr}^2}{M_T^2} \times M_P^3 \quad [pc^3] \tag{8} $$

According to Tabachnik & Tremaine (2002), the probability for a "suitable" star to have a planet in the mass and period ranges $[M, M + dM]$ and $[T_d, T_d + dT_d]$ is given by:

$$ P(T_d, M)\, dT\, dM \approx \frac{C}{T_d\, M_P} \times (M_0/M_P)^\alpha \times (T_{0,d}/T_d)^\beta\, dT\, dM , \tag{9} $$

where the periods are expressed in days, $M_0 = 1.5 M_J$, $T_{0,d} = 90$ days, $C = 1.94 \times 10^{-3}$, $\alpha = 0.11$ and $\beta = -0.27$. About 60% of MS stars (Udry et al. 2000) are suitable for planet detection via radial velocity techniques. However, because we are dealing with proper-motion selection, this factor need not be applied here. The total number of planets then equals the integral of V_P and $P(T, M)$, multiplied by the stellar density (ρ_*):

$$ N_P \approx f(M_V, V(\delta x_0))\, \rho_* \int_0^{T_{max}} dM \int dT\, V_P(T, M) \times P(T, M) \tag{10} $$

$$ N_* \approx N_P / (\int dT\, dM P(T, M)) \tag{11} $$

$$ d_* \approx \left(\frac{3\, N_*}{4\,\pi\,\rho_*} \right)^{1/3} , \tag{12} $$

where the integration boundary T_{max} follows from eqn. (7) and with d_{25pc} set to the limiting astrometric distance[18]. N_* is the number of stars that need be sampled to detect N_P planets, while these N_* stars are located within d_* pc from the Sun. The factor $f(M_V, V(\delta x_0))$ is less or equal than unity, and depends on the absolute magnitude of the target stars and the apparent magnitude at which the astrometric accuracy of δx_0 is achieved[19].

We summarize the results in Table 5, where we break down the expected number of planets according to the spectral type of the host star and the range of the planetary companion. This information is presented for two confidence levels: 10σ (4.5σ) for the top (bottom) part of the table. Several points are noteworthy: 1) A large number of extra-solar giant planets (EGPs) can be reliably (10σ) detected by FAME; 2) about 90, 130 and 1,300 for the mass ranges [0.1–10], [10–20] and [20–80] M_J, respectively; 3) lowering the required detection threshold mainly increases the number low-mass planets; 4) the smallest detectable planetary mass is smaller for less massive MS stars. The latter is due to the much larger abundance of low-mass stars (factor 25 from FV to MV). Overall, we expect that FAME will discover $\sim 1,500$ (2,000) EGPs at the 10σ (4.5σ) level around stars brighter than $V = 10$. For Gaussian statistics, 99.99932% of 4.5σ detections are real, resulting in ~ 0.5 false detections.

It is important to note that the above estimates are lower limits since we are only considering stars brighter than $V = 10$, where the astrometric accuracy is optimal. For example, the astrometric accuracy is about twice worse at $V = 11$, but the volume sampled about 60% larger. As a result, many more planets can be detected in the more distant environs, but only those that are massive enough to cause the larger astrometric signal[20].

1.2.5. Galactic, Extragalactic and Cosmological Implications

After the stellar ages have been established for the 0.5% sample, the evolution of Galactic properties are "easily" reconstructed: for example, the star-formation history of the Milky Way would follow from the number of stars as a function of age, for those stars that have a MS lifetime that exceeds the age of the Galactic disk (late-G and K-type stars). The

---

[18]That is to say, d_{lim} is the distance at which a star of given absolute luminosity reaches the apparent magnitude for which astrometry with error δx_0 can be achieved.

[19] The total number of stars surveyed that yield N'_P planets equals $N'_* = N'_P/(\int dM\, dT P(T, M))$. These stars are located in a region within $d'_* = [3\, N'_*/(4\pi\rho_*)]^{1/3}$ pc. We associate d'_* with the distance limit of the planet survey. However, the required astrometric accuracy of δx_0 μas can only be achieved for stars brighter than $V = V(\delta x_0)$. For FAME, with $\delta x_0 = 50$ μas, $V(\delta x_0) \approx 10$. Thus, intrinsically bright stars can be surveyed to larger distances ($d_{V=10}$) than faint stars. If d'_* exceeds $d_{V=10}$, the depth of the planet survey is restricted to $d_{V=10}$. Finally, we can determine $f(M_V, V(\delta x_0)) = MAX(d_{V=10}/d'_*, 1)^3$.

[20]We find +470 at 10σ, and +1,300 at 4.5σ

large number of thin-disk and thick-disk stars in the 0.5% sample ensures that the formation history of both major components of the Milky Way can be unambiguously reconstructed[21].

With the aid of the proper motions of the 0.5% sample, one may even be able to uncover evidence of Galactic cannibalism (Helmi, White, de Zeeuw, & Zhao 1999). Cold Dark Matter (CDM) galaxy formation scenarios predict (Moore *et al.* 1999) a large number of dark matter clumps, which could have been the seeds of dwarf galaxies. Such CDM-dwarfs may have been tidally disrupted to form "halo streamers:" a very useful tool to study the extent, shape and evolution of the dark matter halo of the Milky Way [e.g., Zhao *et al.* (1999); Helmi & de Zeeuw (2000); Harding *et al.* (2001)]. In fact, detailed simulations by Helmi & de Zeeuw (2000) estimate that FAME would be able to detect 15% of all halos streamers that pass through the solar neighborhood. However, this may be an underestimate because halo streamer may be more prevalent towards the Galactic plane since, in an oblate dark matter halo (Olling & Merrifield 2000), many of them may "sink" towards the disk due to dynamical friction and differential precession (Tremaine & Ostriker 1999; Peñarrubia, Kroupa, & Boily 2002).

Thus, the 0.5% sample will revolutionize our understanding of the physics of stars, the formation history of the thin and thick disks, as well as the evolution of the Helium fraction and the metallicity. Although FAME is not designed with these particular applications in mind, this sample holds enormous promise to contribute significantly to the major questions in galaxy formation and cosmology.

In summary, with the delivery of the FAME 0.5% sample, astrophysicists will find themselves in the unusual situation that inconsistencies between theory and observation can no longer be blamed on inaccurate distances. In the after-FAME era, the astrophysical interpretation of the FAME data will be limited by the availability of high-quality spectro-photometric data. A DISCOVERY-class implementation of FAME, equipped with a 6–8 band photometric system goes a long way towards obtaining the data required for the precise inference of astrophysical quantities. After all, the stellar physical parameters can be determined very well from high-S/N intermediate-band photometry [e.g., Bailer-Jones (2000); Olling (2001)].

1.3. Degraded Astrometric Performance

The science that a space astrometric mission can accomplish at 100 μas is excellent while that at 200μas is well worth doing. The sample of stars with the best astrometry is reduced by a factor of eight for 100 μas accuracy and by 64 for 200μas accuracy in comparison with the FAME mission. In comparison to the Hipparcos mission, 200μas accuracy give a factor

---

[21]To obtain more spheroid stars, one may relax the distance criterion: distance limits of 0.5%, 1%, 2%, 5% and 10% yield 0.2k, 0.8k, 2.5k, 13.4k and 31k halo stars, respectively.

of five in accuracy for 9th magnitude stars with the sample of stars increased by 125 for halo stars and 25 for stars in the disk. Further observations of stars as faint as 15th magnitude will be made whereas Hipparcos plus Tycho measured stars as faint as 12th magnitude.

For the low precision samples, with a limiting distance larger than the disk thickness, the sample size decreases only by factors of four and eight for 100 μas and 200μas, respectively. A reduced astrometric performance will most strongly affects those programs that depend on parallax measurements for distant stars [compare Table 1 with Tables 3 and 4]. For example, at 100 (200) μas, the Cepheid and K-giant samples will reach to only 1000 (500) pc and 600 (300) pc, respectively. At 100 μas, the Galactic rotation curve and the vertical density profile can still be established, but only marginally. At 200 μas, these studies will be severely hampered by the difficulties associated with the interpretation of low-fidelity, or even negative, parallaxes [e.g., the Lutz-Kelker bias Lutz & Kelker (1973); Oudmaijer, Groenewegen, & Schrijver (1998)].

1.3.1. Distance Scale

The calibration of the distance scale can be accomplished in many ways. Determining the absolute magnitude of Cepheids, RR Lyrae stars, subdwarf stars, open clusters, and statistical parallaxes. Significant results can be obtained at 100 and 200 μas accuracies.

For example in determining the calibration of the distance scale from Cepheids, the dominant source of error is the uncertainty in interstellar extinction since they lie in the galactic plane. This error is estimated to be 0.04 mag in B-V (FAME, Science Requirements Document). For 100 μas accuracy, the error in the zero point is estimated to be 0.013 for all Cepheids observed and 0.027 for those Cepheids with periods greater than 10 days. For 200 μas accuracy the zero point is estimated to be determined to 0.022 for all Cepheids and 0.046 for those with periods greater than 10 days.

Parallaxes of nearby RR Lyre stars will be used. For the 73 RR Lyrae stars which FAME will determine a 10% distance, the mean absolute magnitude can be determined to an accuracy of 0.022 mag. Degrading the astrometric accuracy to 100 and 200 μas will result in a mean absolute magnitude accuracy of 0.031 and 0.04 mag respectively.

For subdwarf stars too, parallax errors of better than 10% are required. The number of stars with $[Fe/H] \leq 1.5$ that meet this requirement for the FAME mission accuracy of 50 μas accuracy is 700. The number of stars falls off inversely as the distance cubed. This is tolerable for an accuracy of 100 μas ($N_{SD,100\mu as} \sim 90$) but would be terrible for 200 μas ($N_{SD,100\mu as} \sim 11$) because a smaller number of subdwarfs will significantly limit the accuracy of the calibration of theoretical evolutionary tracks. However, a FAME with reduced

astrometric accuracy would still be important as its proper-motion survey would lead to the discovery many nearby faint, cool, low mass, high velocity, metal poor subdwarfs.

Open clusters using the main sequence fitting technique have been used to determine the distance scale. There are discrepancies in the distance to the Pleiades, Praesepe and Coma clusters whose MS-fitting distances disagrees with the Hipparcos distances. This discrepancy will be resolved either vindicating the Hipparcos distance scale or determine new more reliable distances, free from Hipparcos' systematic errors.

Statistical parallaxes require proper motion precisions of about 20 km/s at 3 kpc or 1.4 mas/yr at V = 13 mag. This will be achieved with a proper motion accuracy of 200 μas/yr at an apparent magnitude of 9.

1.3.2. Mass and Luminosity Calibration of Solar Neighborhood Stars

The calibration of the luminosities of stars will be improved by a factor of 10^2 to 5^2 over Hipparcos for astrometric accuracies of 100 and 200 μas, respectively. For V=9, these accuracies lead to a fractional parallax error of 10% at distances of 0.5 and 1 kpc for 200 and 100 μas, respectively. For bright massive supergiants, it is estimated from the luminosity function that 30–230 such stars lie within 1 kpc. The mean absolute magnitude will be determined to 0.03 and 0.04 mag for astrometric accuracies of 100 and 200 μas respectively. There will be about 15,000 supergiants and 400,000 giant stars with $M_V \leq 0.5$ in the HR diagram brighter than $V = 10$. With this large number of stars, it will be possible to calibrate the mean absolute magnitudes of groups of stars in the upper part of the HR diagram. The largest source of confusion in this process of luminosity calibration is the interstellar extinction.

Significant contributions will be made to our knowledge of the mass luminosity relation by enabling determination of the masses of individual components in numerous binary systems. If the stars are not too distant, FAME will detect almost all binaries with periods $5 \leq T \leq 5$ years from the observed wobble of the photocenter. At 50 (100) [200] μas accuracy, the search would yield only 228k (74k) [9k] stars within 100 (50) [25] parsec. Given the limited amount of ground-based telescope time, only the most interesting systems will be followed up with radial-velocity measurements to determine the individual stellar masses.

Follow-up observations of the 1×10^6 eclipsing binaries that will be discovered via FAME photometry will be even more important. After all, for these systems the radii (gravities) will also be known so that the models of stellar evolution will be observationally very well-constrained. Note that this aspect of the FAME mission is independent of the achievable astrometric accuracy.

1.3.3. Brown Dwarfs and Planets

In section 1.2.4 we performed detailed calculation that indicate about 2,200 (3,500) extra-solar giant planets will be detected at the 10σ (4.5σ). We also showed that the total number of EGPs detected by a FAME mission is essentially independent of astrometric accuracy. This curious result is due to the fact that, as the accuracy decreases, the magnitude limit and hence the number of surveyed stars increases. However, the average mass of the EGP increases as astrometric performance worsens, while the dominant spectral type changes[22] from F to F/G to K when the accuracy decrease from 50 to 200 μas.

1.3.4. Star Forming Regions

Star forming regions are found beyond 100 pc, the distance Hipparcos measured parallaxes to 10% accuracy. Astrometric accuracies of 100 and 200 μas will allow the investigation of star forming regions at distances of 1 and 0.5 kpc respectively. This allows studies of the nearby low mass star forming regions such as Taurus-Auriga at 150 pc as well as regions of intense star formation such as Orion at 450 pc. Massive star forming regions such as S 106, NGC 7538 are at distances of 1 kpc. An astrometric mission will not only determining the distances to star forming regions but also from the combination of parallax and proper motions also determine the kinematics of these regions. It will allow the three dimensional structure of these regions to be studied. It will further the study of pre-MS stars.

1.3.5. Other Studies

There are many other areas of astrophysics that will be significantly impacted by an astrometric space mission. These range from the discovery of nearby loose associations from proper motion data, photometric detection of stellar companions, establishment of a fundamental optical reference frame, statistics on almost all type of stars such as white dwarfs, planetary nebulae, subdwarf O and B stars, et cetera. Many of these areas depend on FAME's photometric capabilities, the positional accuracy at faint magnitudes or the proper-motion precision, and are hence fairly insensitive to a degradation of astrometric performance. We list some of those studies in the next two sections.

At faint magnitudes, the astrometric precision quickly becomes rather poor because

---

[22]For 4.5σ detections, about 16% (21%) of EGPs will be found with masses below 10 (20) M_J at 50 μas. These fractions decrease to 5% (6%) and 16% (6%) at 100 μas and 200 μas, respectively. The larger number of low-mass planets in the 200 μas-astrometry sample arises from the fact that the mass of the primary is 49% smaller in this sub-sample.

FAME moves from the photon-statistics regime ($\delta x_0 \propto 1/\sqrt{N_{phot}}$) to the readnoise-dominated regime ($\delta x_0 \propto 1/N_{phot}$). At V=15, 16, 17, and 18, we estimate that FAME can achieve astrometric accuracies of 0.3, 0.6, 1.2, and 2.7 mas (Olling FTM2001-14).

1.3.6. Science at 1000 μas: Nearby Stars

These accuracies seem fairly poor, except for nearby stars with large parallaxes. For example, a V=18 star at 37 parsec would still have its distance measured to 10%. Such star would have an absolute magnitude of $M_V \sim 15.2$, or $L/L_\odot \sim 10^{-4}$. Thus, FAME could be used to obtain accurate parallaxes for faint nearby stars (Salim, Gould & Olling 2002). because the size of the FAME catalog is bandwidth limited, not all faint stars can be included in the target list. However, at high Galactic latitude, where the star density is substantially smaller, the magnitude limit could be relaxed[23] without significantly affecting the downlink requirements.

Thus, the solar neighborhood could be mapped out with great precision down to the faintest known stars: white dwarfs (WDs) and low-mass main-sequence stars. These components contribute significantly to the total stellar mass density: a firm determination of those mass densities is highly desirable [e.g., Bahcall (1984a,b); Kuijken & Gilmore (1989a,b); Holmberg & Flynn (2000)].

White dwarfs have also been used extensively to obtain estimates for the age of the stellar disk [e.g., (Liebert, Dahn, & Monet 1988), and references therein and thereto], via the turnover in the luminosity function. This turnover occurs just beyond $L/L_\odot \sim 10^{-4}$ where the density is about 10^{-3} per pc^3 per magnitude García-Berro *et al.* (1999), or about 200 within 37 pc. The space density is reputed to drop by a factor of ten at $L/L_\odot \sim 3 \times 10^{-5}$ ($M_V \sim 16$). For $V \lesssim 18$, FAME will obtain **20%** distances within $d = 50$ pc, so that we expect 56 such WDs on the whole sky: an increase of a factor of ten with respect to the current value (Knox, Hawkins, & Hambly 1999).

Note that the accuracy in the parallax can be relaxed quite a bit to find more nearby stars. Ground-based observing campaigns can obtain 1 mas accuracy, but only for a limited number of (interesting) objects (Dahn *et al.* 2002; Monet *et al.* 1992).

---

[23]To, for example, V=18 for 25% of the sky

1.3.7.   Science at 1000 µas: Nearby Galaxies

Extragalactic astronomy is also quite possible with FAME. Though these objects are too distant to determine their *trigonometric* parallaxes reliably, the *rotational* parallaxes could be determined for the Magellanic Clouds. This technique employs the large-scale rotational motion and the measurements of three of its projections (radial and tangential) to determine the systemic components, inclination, rotation speed and distance (Olling & Peterson 2000). In order to do so, the components of non-circular motion (Olling & Peterson 2000) and even a time-variable inclination need be incorporated in the analysis (van der Marel *et al.* 2002). Thus, FAME data will enable detailed kinematical studies of our own galaxy, as well as investigations of the nearest external galaxies. Extrapolating from past experience, we expect that the synergy of detailed MW studies, and the panoramic picture offered by the external systems will greatly enhance our understanding of spiral galaxies as a class of objects.

The errors on the individual stellar proper motions delivered by FAME are just a bit too large, but this low precision is compensated-for by the large numbers of LMC stars. Star counts in the region of the LMC indicate that there are at least 40,000 LMC members down to $R = 16$, within 8 degrees of the LMC center [Olling (2002), private communications]. The expected maximal "rotational signature" is of order 55 $\mathrm{km\,s^{-1}}$ at 50 kpc, or about 0.23 $\mathrm{mas\,yr^{-1}}$. The systemic motion is about four times larger. At 0.6 mas accuracy, the internal motions are detected at the 0.3σ level, per star. If root-N statistics hold, the internal motion of the LMC can be detected at the $\leq 0.23/(0.6 \times \sqrt{40,000}) \sim 3\,\mu\mathrm{as\,yr^{-1}} \sim 76\sigma$ level. Here we assume that the other model parameters that need to be determined are "orthogonal" to the internal motion. This can be accomplished by expanding the galaxian velocity field in Fourier series (Olling & Peterson 2000). Application of the root-N scaling law requires that the FAME catalog is free from systematics at the 3 μas level, while FAME's reference frame is designed to only 50 μas. Despite this apparent problem, the systematics of the FAME catalog could improve the accuracy to about 7 μas by incorporating about 10^6 faint QSOs into the catalog (Salim, Gould & Olling 2002). In this case, the accuracy of the attainable LMC kinematics is reduced by a factor of two over the above estimate: still a very good result indeed.

1.4.   Milli-Magnitude Photometry with FAME

FAME will yield photometry in three bands: 1) SDSS r', 2) SDSS i', and 3) the 550–850 nm astrometric band. AT $V = 11$, the photometric accuracy in the astrometric band is about 5 mmag (5×10^{-3}), per observation. The FAME scanning law is such that, on average, FAME observes each star during 77 ± 31 independent "epochs" of 2 ± 1 hours duration, while about 24 observations are gathered during the 2 hour batches. The independent epochs are

separated by 10^{+30}_{-9} days. Since FAME uses just one CCD per SDSS band, the photometric observations in the SDSS bands are ten times less frequent than in the astrometric band, or about two per 2-hr batch per band. The accuracy will be $\sim$9 mmag per observation: good enough to characterize eclipsing binary stars, but is not useful in the area of planetary transits.

The FAME scanning law ensures excellent temporal coverage for events that repeat at timescales of order 10 days. Furthermore, FAME has a large "diurnal field of view:" on a typical day, FAME will observe about 20% of the sky. In combination with the excellent sensitivity and the fairly large magnitude range, the FAME data would present the best opportunity to launch a study into the temporal behavior of the firmament.

1.5. Planetary Transits Observed by FAME

As an example, we present a simulation of the only transiting planetary system currently known. For this simulation, we assumed a mission duration of 5 years and a launch on 2004/06/15 (other configurations will produce similar results). The band that each viewport maps out on the celestial sphere is recorded and compared with the location and ephemerides of HD 209458b. The results are presented in Figure 3. The top row shows the distribution of the 862 epochs of observation in mission-time and orbital-phase. The histogram of orbital phases (binsize=0.01) shows excellent to fair coverage[24] for periods from 1.75 to 7 days (middle panels). The simulated lightcurves in the bottom panels show similar quality. Due to the scanning law, the temporal coverage of FAME lightcurves is also affected by ecliptic latitude ($\beta \sim 28^o$ for HD 209458), where stars with smaller (larger) β have poorer (better) coverage. For FAME, the length of an observing epoch ($\sim$ 2 hours), more-or-less covers the planetary transit in systems like HD 209458.

Given an edge-on observing geometry, the probability of detecting a hot-Jupiter in transit equals the ratio of the transit time (T_{trans}) to the orbital period (T_{orb}): $P_{det} = T_{trans}/T_{orb}$. Applying the mass-radius relation for Sun-like main-sequence stars, one can estimate that this probability reduces to $P_{transit,seen,once} \approx 0.077\,T_{orb}^{-2/3}$, where T_{orb} is measured in days. The orbital period can be established when the transit is observed during at least two independent epochs. Using our simulations we estimate this probability[25] to be: P_{2det}=100%, 78%, 53%,

---

[24]Employing a Monte-Carlo simulation with randomized initial phases, we estimate that "HD 209458b" can be observed in transit (39) 24 [15] times, at (10) 6 [3] independent epochs if the period were to equal (1.75) 3.5 [7] days.

[25]Numerically we find: $\ln(P_{2det}) \sim 4.494 + 0.3093 \times \ln(T_{orb}) - 0.1928 \times [\ln(T_{orb})]^2$, where P_{2det} is measured in percent, and T_{orb} in days, and $P_{2det} = 1$ for $T_{orb} \lesssim 2$ days. The probability for multiple detections is also fairly large: systems with three detected transit events occur about half as frequent as systems with two

28%, 15%, 1% for orbital periods of ≤ 2, 7, 14, 30, 365 days, respectively (if the system is edge-on, and has a companion similar to HD 209458b).

Several other factors need to be considered. In doing so, we follow the prescriptions used for the *Kepler* mission (*Kepler* 2001). For this mission, it is estimated that 45% of stars are amenable to planetary-transit detection ($P_{*,OK}^K \sim 0.45$). The remaining stars are either giants (too large/small effect) or too variable ("drowned in noise"). For the FAME catalog we have already culled the giants, so we use $P_{*,OK}^F \sim 0.60$ [c.f., (Udry *et al.* 2000)] The geometric detection probability approximately equals the ratio of the stellar radius and the major axis of the orbit (for circular orbits): $P_G(T) \sim R_*/a \sim 47.5\,T_{orb,days}^{-2/3}$ %, where we have assumed R_* to equal $R_\odot$. The expected number of systems that will have a star in transit is then given by:

$$N_{Trans} = N_* \times P_{*,OK} \int dT\; P_G(T) \times P_P(T) \times P_{det}(T)\,, \qquad (13)$$

where the integral is evaluated over all relevant orbital periods, and N_* is the number of stars surveyed. The probability $[P_P(T)]$ that an F–K main-sequence star has a giant planet is taken from Tabachnik & Tremaine (2002) (see also eqn. (9) above). In Table 5 we estimate the number of stars showing transits for the FAME and *Kepler* missions. We assume that *Kepler* will survey $N_*^K = 2.2 \times 10^5$ down to V=14, while FAME will measure $N_*^F = 7.6 \times 10^5$ stars between $R=9$ and 11.

From Table 5 it follows that the expected number of objects N_{trans}^i is a sensitive function of P_G and P_P. In evaluating N_{Trans}^i, we have integrated over the full probability density distribution. We conclude that a FAME-like mission would detect about 365 "hot Jupiters" in transit, or about three times more than the estimated number for the "*Kepler*" mission. Of course, the *Kepler* mission can detect much fainter transit signals, and even the waning and waxing of ~ 900 short period EGPs that are *not* in edge-on orbits. On the other hand, most of the FAME detections would occur around bright stars ($V \lesssim 11$), while most *Kepler* detection occur for $V = 14$ stars (~ 16 times fainter). Thus, the FAME EGPs are suitable targets for follow-up observations with instruments such as SIM or TPF, as well as sensitive, high-resolution spectroscopy.

---

observed transits.

REFERENCES

Adams, J.D., *et al.*2001, AJ, 121, 2053

"Allen's Astrophysical Quantities," 2000, 4th Edition, Eds. Cox, A.N., Springer-Verlag

Andersen, J., 1991, A&AR, 3, 91

Bertelli, G., Bressan, A., Chiosi, C., Fagotto, F., & Nasi, E. 1994, A&AS, 106, 275

Bailer-Jones, C.A.L., 2002, Ap&SS, 280, 21

Bailer-Jones, C.A.L., 2000, A&A, 357, 197

Binney, J., Merrifield, M.R., 1998, Galactic Astronomy, Princeton University Press, Princeton,NJ

Bahcall J.N., 1984a, ApJ, 276, 156; 1984b, ApJ, 276, 169

Chiang, E. I., Tabachnik, S., & Tremaine, S. 2001, AJ, 122, 1607

Crézé M., Chereul E., Bienaymé O., Pichon C., 1998, A&A, 329, 920

Dahn, C. C. et al. 2002, AJ, 124, 1170

Dehnen W., Binney J., 1998, MNRAS, 298, 387

Duquennoy, A. & Mayor, M. 1991, A&A, 248, 485

Kaluzny, J., *et al.*, 1998, AJ, 115, 1016

Eisner, J.A., Kulkarni, S.R., 2002, ApJ, 574, 426

Eisner, J. A. & Kulkarni, S. R. 2001, ApJ, 561, 1107

FAME, 2000-2002, The FAME team. eg., at http://www.usno.navy.mil/FAME/

Feast M., Whitelock P., 1997, MNRAS, 291, 683

Fitzpatrick, E.L., *et al.*2002, ApJ, 564, 260

Flynn C., Fuchs B., 1994, MNRAS, 270, 471

García-Berro, E., Torres, S., Isern, J., & Burkert, A. 1999, MNRAS, 302, 173

García-Sánchez, J., *et al.*, 2001, A&A, 379,634

Gould, A., 2000, ApJ, 528, 156

Gray, R. O., Graham, P. W., Hoyt, S. R., 2001, AJ, 121, 2159

Harding, P., *et al.*, 2001, AJ, 122, 1397

Han, I., Black, D. C., & Gatewood, G. 2001, ApJ, 548, L57

Helmi, A., de Zeeuw, P.T., 2000, MNRAS, 319, 657

Helmi, A., White, S. D. M., de Zeeuw, P. T., & Zhao, H. 1999, Nature, 402, 53

Holmberg, J. & Flynn, C. 2000, MNRAS, 313, 209

Kepler, 2001, http://www.kepler.arc.nasa.gov/

Knox, R. A., Hawkins, M. R. S., & Hambly, N. C. 1999, MNRAS, 306, 736

Kuijken K. & Gilmore G., 1989a, MNRAS, 239, 571; 1989b, MNRAS, 239, 605

Kurucz, R. 2001, astro-ph/0105400

Lebreton, Y., 2001, ARA&A, 38, 35

Lebreton, Y., Perrin, M.N., Cayrel, R., Baglin, A., Fernandez, J., 1999, A&A, 350, 587

Liebert, J., Dahn, C. C., & Monet, D. G. 1988, ApJ, 332, 891

Lutz, T. E. & Kelker, D. H. 1973, PASP, 85, 573

van der Marel, R. P., Alves, D. R., Hardy, E., & Suntzeff, N. B. 2002, AJ, 124, 2639

Mason, B. D., Wycoff, G. L., Hartkopf, W. I., Douglass, G. G., & Worley, C. E. 2001, AJ,
    122, 3466

Mayor M., 1974, A&A, 32, 321

Monet, D. G., *et al.*, 1992, AJ, 103, 638

Moore, B., *et al.*, 1999, ApJ, 524, L19

Olling, R.P.,2000–2001, Fame Technical Memorandums at
    http://ad.usno.navy.mil/∼olling/FAME/rpo_fame.htm

Olling, 2001, FTM2001-03, http://ad.usno.navy.mil/∼olling/FAME/FTM2001-03.ps

Olling, 2001, FTM2001-07, http://ad.usno.navy.mil/∼olling/FAME/FTM2001-07.ps

Olling, 2001, FTM2001-14, http://ad.usno.navy.mil/∼olling/FAME/FTM2001-14.ps

Olling, 2001, FTM2001-15, http://ad.usno.navy.mil/∼olling/FAME/FTM2001-15.ps

Olling, R. P. & Merrifield, M. R. 2001, MNRAS, 326, 164

Olling, R.P., Peterson, D.M., 2000, astro-ph/0005484

Olling, R. P. & Merrifield, M. R. 2000, MNRAS, 311, 361

Olling R.P., Merrifield M.R., 1998, MNRAS, 297, 943

Oudmaijer, R. D., Groenewegen, M. A. T., & Schrijver, H. 1998, MNRAS, 294, L41

Paczyński, B, astro-ph/9608094

Perryman, M. A. C. *et al.*, 2001, A&A, 369, 339

Peñarrubia, J., Kroupa, P., & Boily, C. M. 2002, MNRAS, 333, 779

Pottasch, S.R., 1996, A&A, 307, 561

Salim, S., Gould, A., Olling, R.P., 2002, ApJ, 573, 631

Sandage, A., Saha, A., 2001, ApJ, 123, 2047

Sneden, C., *et al.*1995, PASP, 107, 997

Snider, S., *et al.*, 2001, ApJ, 562, 528

Söderhjelm, S., 1999, A&A, 341, 121

Soubrian, C., Katz, D. & Cayrel, R., 1998, A&AS, 133, 221

Tabachnik, S. & Tremaine, S. 2002, MNRAS, 335, 151

Tremaine, S. & Ostriker, J. P. 1999, MNRAS, 306, 662

Udry, S., Mayor, M., *et al.*, 2000, A&A, 356, 590

Wyithe, J.S.B. & Wilson, R.E., 2002, ApJ, 571, 293

Zhao, H., Johnston, K. V., Hernquist, L., & Spergel, D. N. 1999, A&A, 348, L49

Table 1: Estimated contents of the FAME catalog. The columns list: $\mathbf{1}^{th}$) Spectral type, $\mathbf{2}^{nd}$) Absolute magnitude in the V band, $\mathbf{3}^{rd}$) distance at which the apparent magnitude equals $R = 15$, assuming an average extinction of 1.4 mag per kpc in the V band, $\mathbf{4}^{th}$) the total number of stars, $\mathbf{5}^{th}$) 10σ limiting distance ($=$ MIN$[d(\Delta\pi/\pi = 0.1), d(R = 15)]$), $\mathbf{6}^{th}$) apparent R magnitude at $d = d_{10\%}$, $\mathbf{7}^{th}$) estimated number of stars (in multiples of 1,000) in the thin disk, $\mathbf{8}^{th}$) number of stars in the thick disk, $\mathbf{9}^{th}$) number of stars in the spheroid, $\mathbf{10}^{th}$–$\mathbf{14}^{th}$, same as 5th–9th, but then for stars with a 200σ parallax determination. **Note: the results contained in this table are based on the old/wrong star-count model, but the numbers are approximately correct.**

1	2	3	4	5	6	7	8	9	10	11	12	13	14
SPT	M_V	d^{R15}	N_{tot}	$d_{10\%}$	$R_{10\%}$	N_{D1}	N_{D2}	N_S	$d_{0.5\%}$	$R_{0.5\%}$	N_{D1}	N_{D2}	N_S
	mag	pc	1k	pc	mag	1k	1k	1k	pc	mag	1k		
Cep	-4.0	5,356	12	2,000	9.1	1.6	-	-	100	2.5	0.002	-	-
BV	-1.2	3,487	400	1,468	11.2	84	-	-	100	3.9	0.2	-	-
AV	1.9	1,811	1,680	860	12.3	366	-	-	100	6.8	2.6	-	-
FV	3.5	1,166	8,280	649	12.8	2,098	-	-	100	8.2	26.6	-	-
GV	5.1	694	11,120	469	13.4	3,593	375	9.4	100	9.7	87.3	3,641	91
KV	7.4	290	3,760	302	14.1	1,894	127	3.2	81	11.0	57.9	2,414	60
MV	8.8	96	2,280	178	14.9	2,162	86	2.1	50	12.0	44.7	1,862	46
rest	0.6	2,452	12,436	1,209	11.6	2,408	408	16.2	100	5.1	8.9	370	9
TOT			40,000			12,600	996	31			228	8,300	206

Table 2: The Expected number of giant planets broken down according to spectral type of the primary, the mass of the planet and the confidence level of the detection. The 1th and 2nd columns list the spectral type and the average stellar mass. The confidence level, the minimum planetary mass and the mass range of the planets are tabulated in columns #3, #4 and #5, respectively. Columns #6 — #9 list the probability of finding a planet in the mass range listed in column #5 (with 2 days $\leq T \leq 10$ year), the number of planets, the number of stars in the sample, and the maximum distance, respectively. For the stellar densities, we used: $\rho_{*,FV} = 2.5$, $\rho_{*,GV} = 6.3$, $\rho_{*,KV} = 10$, $\rho_{*,MV} = 63$ stars per 1000 pc^{-3} [cf., Binney & Merrifield (1998), table 3.19]. The number of stars sampled is limited by the $f(M_V, V(\delta x_0))$ factor in case the d_{max} values are negative (see footnote 19 for details). **Note: the results contained in this table are based on the old/wrong star-count model, but the numbers are approximately correct.**

1	2	3	4	5	6	7	8	9
SPT	M_T	$a_{P,\sigma}$	$M_{P,min}$	M_P	P_P	N_P	N_*	d_{max}
	[$M_\odot$]	[σ]	[M_J]	[M_J]	[10^{-3}]			[pc]
FV	1.26	10	6.60	0.1–10	81	3.4	42	15.8
GV	0.95	10	3.95	0.1–10	81	15.0	185	19.1
KV	0.63	10	2.55	0.1–10	81	54.0	667	25.1
MV	0.20	10	0.61	0.1–10	81	20.8	256	-9.9
FV	1.26	10		10–20	9	21.7	2,414	61.2
GV	0.95	10		10–20	9	96.1	10,666	73.9
KV	0.63	10		10–20	9	12.8	1,425	-32.4
MV	0.20	10		10–20	9	2.3	256	-9.9
FV	1.26	10		20–80	16	953.2	59,240	-177.9
GV	0.95	10		20–80	16	311.0	19,331	-90.1
KV	0.63	10		20–80	16	22.9	1,425	-32.4
MV	0.20	10		20–80	16	4.1	256	-9.9
Tot		10		0.1–10		93.2	1,150	
Tot		10		10–20		132.9	14,761	
Tot		10		20–80		1,291.2	80,252	
Tot		10		0.1–80		1,508.3	80,252	
FV	1.26	4.5	2.88	0.1–10	81	37.2	459	35.2
GV	0.95	4.5	1.70	0.1–10	81	164.5	2,031	42.5
KV	0.63	4.5	1.11	0.1–10	81	115.4	1,424	-32.4
MV	0.20	4.5	0.27	0.1–10	81	20.8	256	-9.9
FV	1.26	4.5		10–20	9	238.8	26,490	136.0
GV	0.95	4.5		10–20	9	174.2	19,331	-90.1
KV	0.63	4.5		10–20	9	12.8	1,425	-32.4
MV	0.20	4.5		10–20	9	2.3	256	-9.9
FV	1.26	4.5		20–80	16	953.2	59,240	-177.9
GV	0.95	4.5		20–80	16	311.0	19,331	-90.1
KV	0.63	4.5		20–80	16	22.9	1,425	-32.4
MV	0.20	4.5		20–80	16	4.1	256	-9.9
Tot		4.5		0.1–10		337.9	3,433	
Tot		4.5		10–20		428.1	40,323	
Tot		4.5		20–80		1,291.2	80,252	
Tot		4.5		0.1–80		2,057.2	80,252	

Table 3: Estimated contents of the FAME catalog at **10% astrometric accuracy**. The effects of a degradation of the astrometric accuracy is presented: A) the limiting distance decreases with worse astrometry (columns #3, #7, and #11), and B) the number of stars decreases. The columns list: **1**[th]) Spectral type, **2**[nd]) Absolute magnitude in the V band, **3**[rd]–**6**[rd] for **50** μas astrometry, limiting distance, and the number of stars in the thin-disk stars, thick disk and spheroid, respectively. **7**[rd]–**10**[rd] same as for 3rd–6rd but for **100** μas astrometry. **11**[rd]–**14**[rd] same as for 3rd–6rd but for **200** μas astrometry. **Note: the results contained in this table are based on the old/wrong star-count model, but the numbers are approximately correct.**

1	2	3	4	5	6	7	8	9	10	11	12	13	14
SPT	M_V	d_{50}	N_{D1}	N_{D2}	N_S	d_{100}	N_{D1}	N_{D2}	N_S	d_{200}	N_{D1}	N_{D2}	N_S
	mag	pc	1k	1k	1k	pc	1k	1k	1k	pc	1k	1k	1k
Cep	-4.0	2,000	1.6	-	-	1,000	0.39	-	-	500	0.097	-	-
BV	-1.2	1,468	84	-	-	1,000	39	-	-	500	9.8	-	-
AV	1.9	860	366	-	-	860	366	-	-	500	124	-	-
FV	3.5	649	2,098	-	-	649	2,098	-	-	500	1,247	-	-
GV	5.1	469	3,593	375	9.3	469	3,593	375	9.3	469	3,593	375	9.4
KV	7.4	302	1,894	127	3.2	302	1,894	127	3.2	302	1,894	127	3.2
MV	8.8	178	2,162	86	2.1	178	2,162	86	2.1	178	2,162	86	2.1
rest	0.6	1,209	2,408	408	16.2	1,000	1,649	275	9.2	500	415	46	1.2
TOT			12,600	996	31.0		11,000	863	24.0		9,400	634	16

Table 4: Estimated contents of the FAME catalog at **0.5% astrometric accuracy**. The effects of a degradation of the astrometric accuracy is presented: A) the limiting distance decreases with worse astrometry (columns #3, #7, and #11), and B) the number of stars decreases. The columns list: $\mathbf{1}^{th}$) Spectral type, $\mathbf{2}^{nd}$) Absolute magnitude in the V band, $\mathbf{3}^{rd}$–$\mathbf{6}^{rd}$ for **50** μas astrometry, limiting distance, and the number of stars in the thin-disk stars, thick disk and spheroid, respectively. $\mathbf{7}^{rd}$–$\mathbf{10}^{rd}$ same as for 3rd–6rd but for **100** μas astrometry. $\mathbf{11}^{rd}$–$\mathbf{14}^{rd}$ same as for 3rd–6rd but for **200** μas astrometry. **Note: the results contained in this table are based on the old/wrong star-count model, but the numbers are approximately correct.**

1	2	3	4	5	6	7	8	9	10	11	12	13	14
SPT	M_V	d_{50}	N_{D1}	N_{D2}	N_S	d_{100}	N_{D1}	N_{D2}	N_S	d_{200}	N_{D1}	N_{D2}	N_S
	mag	pc	1k			pc	1k			pc	1k		
Cep	-4.0	100	0.002	-	-	50	0	-	-	25	0	-	-
BV	-1.2	100	0.2	-	-	50	0.026	-	-	25	0.003	-	-
AV	1.9	100	2.6	-	-	50	0.33	-	-	25	0.04	-	-
FV	3.5	100	26.6	-	-	50	3.3	-	-	25	0.41	-	-
GV	5.1	100	87.3	3,641	91	50	10.9	455	11	25	1.36	56	1
KV	7.4	81	57.9	2,414	60	50	13.8	576	14	25	1.73	72	1
MV	8.8	50	44.7	1,862	46	50	44.7	1,862	46	25	5.68	236	5
rest	0.6	100	8.9	370	9	50	1.1	46	1	25	0.13	5	0
TOT			228k	8,300	206		74k	2,939	72		9.4k	369	7

Table 5: FAME's capabilities to detect transits of "hot Jupiters," and a comparison with the *Kepler* mission. A total of $N_{*,OK}^K = 0.99 \times 10^5$ and $N_{*,OK}^F = 4.6 \times 10^5$ main-sequence stars are assumed for the Kepler and FAME missions, respectively. The columns list the following: 1th) the range in orbital periods considered; 2nd) The geometrical probability for observing a transit for the upper period listed 3rd) The percentage of stars that have a "hot-Jupiter" in this period range; 4th) The total probability $\int P_G \times P_P \, dT$; 5th) The probability that FAME will detect 2 transit events (weighted by $P_G \times P_P$); 6th) The number of transiting hot-Jupiters to be discovered by FAME $(=N_{*,OK}^F \times \int P_G \times P_P \times P_{2det}^F dT)$; 7th) the assumed detection probability for the *Kepler* mission; 8th) The number of transiting hot-Jupiters to be discovered by *Kepler* $(=N^K \times P_{*,OK}^K \times P_G \times P_P \times P_{det}^K)$; 9th) the FAME-to-*Kepler* ratio of detectable hot-Jupiter transits. **Note: the results contained in this table have NOT been updated to reflect the varying upper limit for the planetary period in eqn. (10), but the numbers are approximately correct.**

1	2	3	4	5	6	7	8	9
T_{orb}^{days}	P_G [%]	$\int P_P$ [%]	$\int P_G \times P_P$ $[10^{-4}]$	$<P_{2det}^F>$ [%]	N_{Trans}^F	P_{det}^K [%]	N_{Trans}^K	$\frac{N_{Tr}^F}{N_{Tr}^K}$
2– 7	12.9	0.26	5.79	93.9	249	100	58	4.29
7– 14	8.2	0.19	2.16	65.8	65	100	22	3.00
14– 30	4.9	0.25	1.78	39.7	33	100	18	1.68
30– 52	3.4	0.21	0.99	20.8	10	100	10	1.00
52–365	1.9	1.07	2.19	5.9	8	100	22	0.36
2–365		1.98	12.92	61.1	365	100	130	2.81

Fig. 1.— The semi-major axis of the photocenter of a pair of main-sequence stars observed from a distance of 100 pc. The size of a_{phot} is calculated according to eqn. (4), where we have expressed its magnitude in units of FAME's astrometric accuracy of 50 μas. Note that we only contoured the part of the diagram where $M_1 \geq M_2$.

Semi−Major axis of Photocentric Motion

Mass of Secondary [M_{SUN}]

Mass of Primary [M_{SUN}]

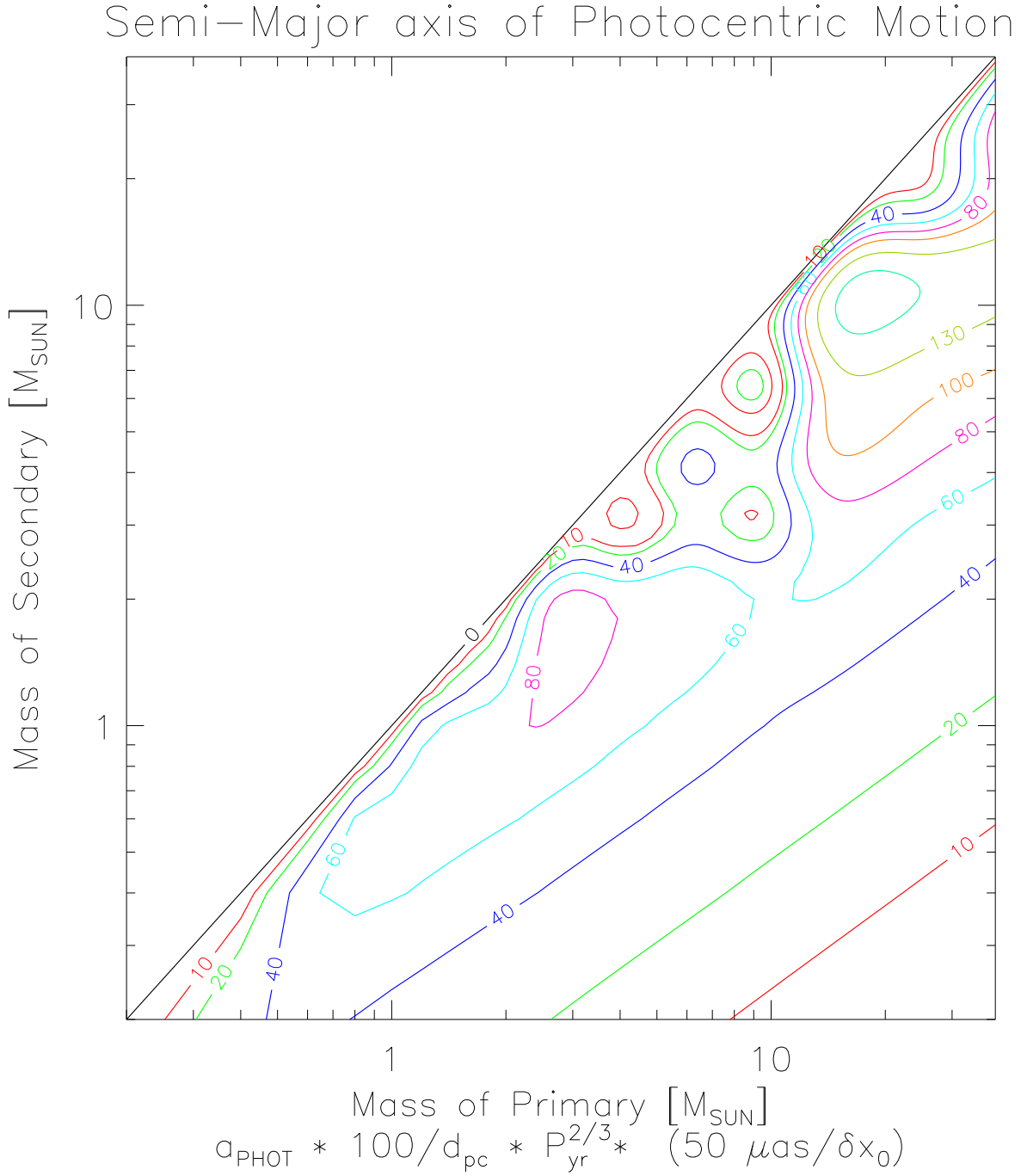$a_{PHOT} * 100/d_{pc} * P_{yr}^{2/3} * (50\ \mu as/\delta x_0)$

Fig. 2.— The semi-major axis of the photocenter of a planet orbiting a main-sequence star, observed from a distance of 25 pc. The size of a_{phot} is calculated according to eqn. (7), where we have expressed its magnitude in units of FAME's astrometric accuracy of 50 μas. The dotted lines of represent lines of constant constant confidence $N \times \sigma$, for the case of a 5 year orbital period, where the N values are associated with the contours. The thick lines are the 10σ detections for periods of 5, 4, 3,2,1 year, from bottom to top.
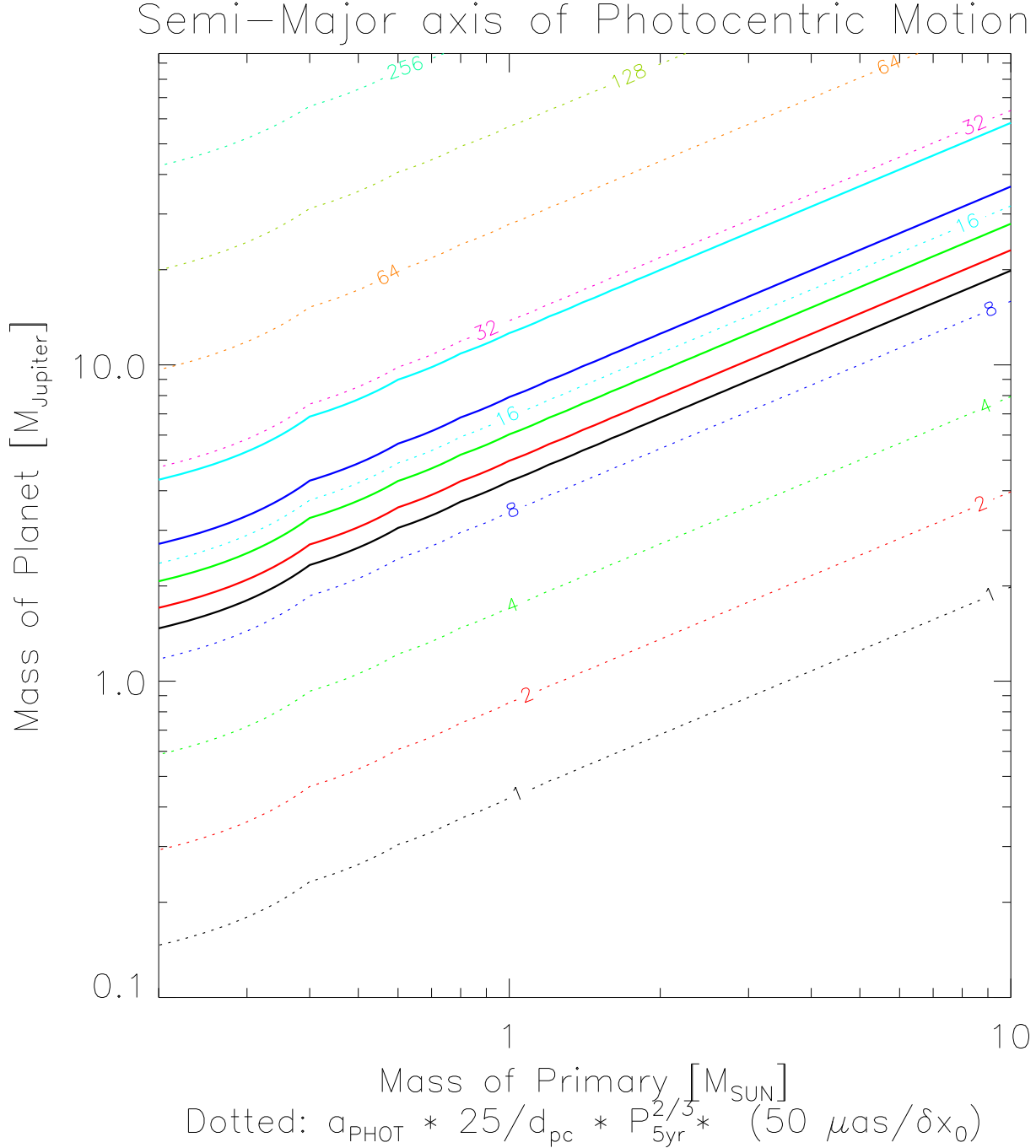
Fig. 3.— Three columns of figures are shown: the middle set is for the actual period of HD 209458b, the left and right for periods twice shorter and longer, respectively. The duration of the transit equals ∼0.1 hours for HD 209458b and is scaled according to the orbital period ($T_{trans} \propto T_{orbit}^{1/3}$). The top row of figures displays the distribution of the observations (crosses) in time and orbital phase. A (red) open square is plotted whenever the "planet" transits the target star. The "vertical" alignment of events occurs when the local precession rate is small. The middle panels indicate that a fairly good coverage of all orbital phases is obtained for $T_{orbit} \sim 7$ days (12 observing epochs during transit events: $N_{TRN} = 12$). The coverage is good ($N_{TRN} = 12$) and excellent ($N_{TRN} = 45$) for $T_{orbit} \sim 3.5$ and 1.75 days, respectively. In these plots, the bold (red) parts of the histograms indicate that a transit occurs. Simulated (phased) lightcurves are presented in the lowest row of plots. As observed for HD 209458b, a depth of 15 milli-magnitude (mmag) is assumed, and a photometric accuracy appropriate for an 11th magnitude stars (3.5 mmag per FP transit). FAME will observe about 10^6 stars with a photometric precision like this or better.